ROBUST GYMNASIUM: A UNIFIED MODULAR BENCHMARK FOR ROBUST REINFORCEMENT LEARNING

Shangding Gu[1*†], **Laixi Shi**[2*], **Muning Wen**[3], **Ming Jin**[4], **Eric Mazumdar**[2],
Yuejie Chi[5], **Adam Wierman**[2], **Costas Spanos**[1]

[1] University of California, Berkeley
[2] California Institute of Technology
[3] Shanghai Jiao Tong University
[4] Virginia Tech
[5] Carnegie Mellon University

ABSTRACT

Driven by inherent uncertainty and the sim-to-real gap, robust reinforcement learning (RL) seeks to improve resilience against the complexity and variability in agent-environment sequential interactions. Despite the existence of a large number of RL benchmarks, there is a lack of standardized benchmarks for robust RL. Current robust RL policies often focus on a specific type of uncertainty and are evaluated in distinct, one-off environments. In this work, we introduce Robust-Gymnasium, a unified modular benchmark designed for robust RL that supports a wide variety of disruptions across all key RL components—agents' observed state and reward, agents' actions, and the environment. Offering over sixty diverse task environments spanning control and robotics, safe RL, and multi-agent RL, it provides an open-source and user-friendly tool for the community to assess current methods and foster the development of robust RL algorithms. In addition, we benchmark existing standard and robust RL algorithms within this framework, uncovering significant deficiencies in each and offering new insights. The code is available at this website.

1 INTRODUCTION

Reinforcement learning (RL) is a popular learning framework for sequential decision-making based on trial-and-error interactions with an unknown environment, achieving success in a variety of applications, such as games (Mnih et al., 2015; Vinyals et al., 2019), energy systems (Chen et al., 2022), finance and trading (Park & Van Roy, 2015; Davenport & Romberg, 2016), and large language model alignment (OpenAI, 2023; Ziegler et al., 2019).

Despite recent advances in standard RL, its practical application remains limited due to concerns over robustness and safety. Specifically, policies learned in idealized training environments often fail catastrophically in real-world scenarios due to various factors such as the sim-to-real gap (Pinto et al., 2017), uncertainty (Bertsimas et al., 2019), noise, and even malicious attacks (Zhang et al., 2020; Klopp et al., 2017; Mahmood et al., 2018). Robustness is key to deploying RL in real-world applications, especially in high-stakes or high-cost fields such as autonomous driving (Ding et al., 2023b), clinical trials (Liu et al., 2015), robotics (Li et al., 2021), and semiconductor manufacturing (Kozak et al., 2023). Towards this, Robust RL seeks to ensure resilience in the face of the complexity and variability of both the physical world (Bertsimas et al., 2019) and human behavior (Tversky & Kahneman, 1974; Arthur, 1991).

Robust RL policies currently fall short of the requirement for broad deployment. Disruptions or interventions can occur at various stages of the agent-environment interaction, affecting the agent's

[*] Equal Contribution.

[†] Technical Report. This work is currently in progress, and we appreciate any constructive comments and suggestions corresponding to *shangding.gu@berkeley.edu* and *laixis@caltech.edu*.

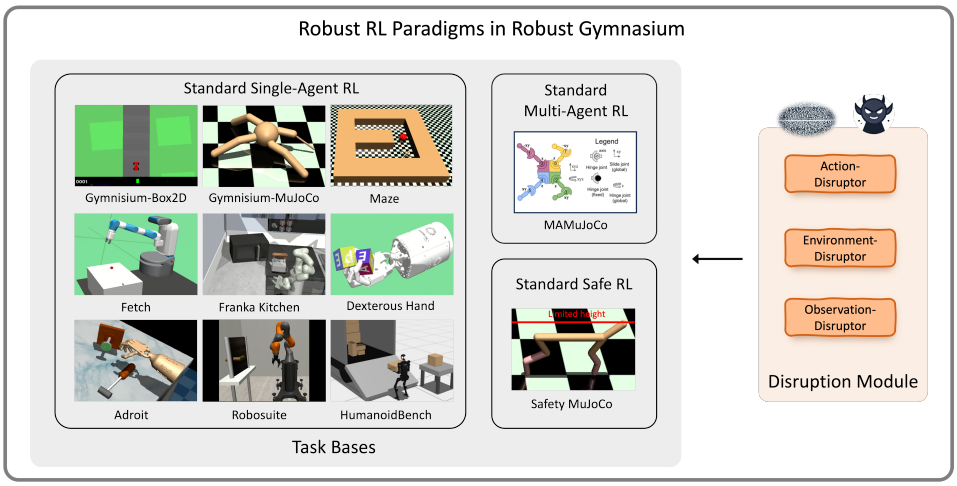

Figure 1: The overview of Robust-Gymnasium. For more details, please visit the website.

observed state (Zhang et al., 2020; 2021b; Han et al., 2022; Sun et al., 2021; Xiong et al., 2022), observed reward (Xu & Mannor, 2006), action (Huang et al., 2017), and the environment (transition kernel) (Iyengar, 2005; Pinto et al., 2017) and existing robust RL policies are vulnerable to such real-world failures (Mandlekar et al., 2017). This vulnerability is, in part, a result of the fact that policies are designed to address only one specific type of disruption (e.g., over the observed state), among other technical limitations (Ding et al., 2024). More critically, robust RL policies are often evaluated in distinct, one-off environments that can be narrow or over-fitted to the proposed algorithms. The absence of standardized benchmarks is a key bottleneck to progress in robust RL. Ideally, a benchmark should offer a wide range of diverse tasks for comprehensive evaluation and account for uncertainty and disruptions over multiple stages throughout the interaction process.

While numerous RL benchmarks exist, including a recent one focused on robustness to environment shifts (Zouitine et al., 2024), none are specifically designed for comprehensively evaluating robust RL algorithms. To address this gap, we present Robust-Gymnasium[1], a unified, highly modular benchmark for robust RL. This open-source tool enables flexible construction of diverse tasks, facilitating the evaluation and development robust RL algorithms. Our main contributions are:

- We introduce a unified framework for robust RL, encompassing diverse disruption types within a modular agent-environment interaction process (detailed in Sec. 2). This framework enables the development of Robust-Gymnasium, a benchmark that comprises over sixty diverse tasks in robotics and control, safe RL, and multi-agent RL; and includes a wide range of disruptions targeting different stages/sources (agent observations, actions, and the environment) with varying modes (e.g., random or adversarial disturbances, environmental shifts) and frequencies. To our knowledge, this is the first unified benchmark specifically designed for robust RL, providing a foundational tool for evaluating and developing robust algorithms.
- We conduct a comprehensive evaluation of several state-of-the-art (SOTA) baselines from standard RL, robust RL, safe RL, and multi-agent RL using representative tasks in Robust-Gymnasium. Our findings reveal that current algorithms often fall short of expectations in challenging tasks, even under single-stage disruptions, highlighting the need for new robust RL approaches. Furthermore, our experiments demonstrate the flexibility of Robust-Gymnasium by encompassing tasks with disruptions across all stages and four disturbance modes, including an adversarial model using a large language model (LLM). This illustrates the potential of LLMs in robust RL research.

[1]Website with the introduction, code, and examples: `https://robust-rl.com/`

2 A UNIFIED ROBUST REINFORCEMENT LEARNING FRAMEWORK

We begin by presenting a robust RL framework that unifies various robust RL tasks explored in the literature, including combinations of these paradigms. We outline the framework in the context of single-agent RL and then extend it to encompass broader classes of RL tasks, such as safe RL and multi-agent RL.

Background: Markov decision process (MDP). A single-agent RL problem is formulated as a finite-horizon Markov decision process (MDP), represented by the tuple $\mathcal{M} = \left(\mathcal{S}, \mathcal{A}, T, P^0, r^0\right)$, where $\mathcal{S}$ and $\mathcal{A}$ denote the (possibly infinite) state and action spaces, and T is the horizon length. The nominal transition kernel $P^0 = \{P_t^0\}_{1\le t\le T}$ defines the environmental dynamics: $P_t^0(s' \mid s, a)$ gives the probability of transitioning from state s to state s' given action a at time step t. The reward function $r^0 = \{r_t^0\}_{1\le t\le T}$ represents the immediate reward at time step t, given the current state s and action a.

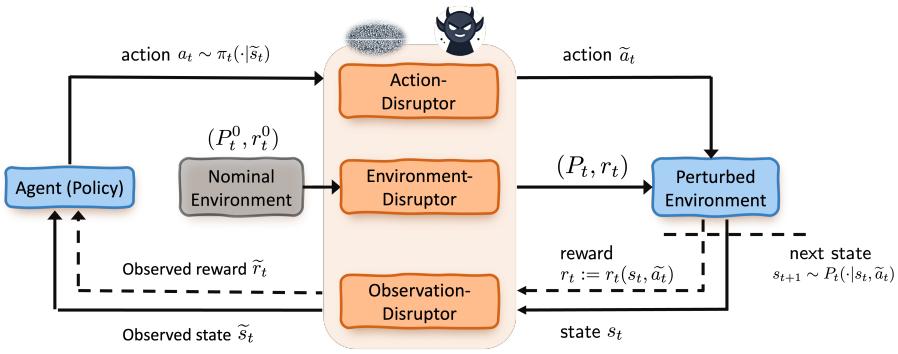

Figure 2: The overview of a finite-horizon MDP with disruptors.

2.1 A UNIFIED ROBUST RL FRAMEWORK: MDPS WITH DISRUPTION

As shown in Fig. 2, a robust RL problem can be formulated as a finite-horizon MDP with an additional disruption module $\mathcal{M}_{\mathsf{dis}} = \left(\mathcal{S}, \mathcal{A}, T, P, r, D_{\mathsf{s}}(\cdot), D_{\mathsf{r}}(\cdot), D_{\mathsf{a}}(\cdot)\right)$, consisting of three potential disruptors (abbreviated as Disrupted-MDP) that affect different components: the *observation-disruptor*, with functions $D_{\mathsf{s}}(\cdot)$ and $D_{\mathsf{r}}(\cdot)$, perturbs the agent's observations (states and rewards); the *action-disruptor* perturbs actions using function $D_{\mathsf{a}}(\cdot)$; and the *environment-disruptor*modifies the environment, resulting in a shifted transition kernel P and reward function r. Further details on the disruptors are provided in the next subsection.

The interaction process between an agent and an MDP with disruption (Fig. 2) unfolds as follows: at each time step $t \in [T]$, the (possibly perturbed) environment outputs the current state s_t and reward r_t. The *observation-disruptor* then perturbs these, sending the modified state $\widetilde{s}_t = D_{\mathsf{s}}(s_t)$ and reward $\widetilde{r}_t = D_{\mathsf{r}}(r_t)$ to the agent. Based on these, the agent selects an action $a_t \sim \pi_t(\cdot \mid \widetilde{s}_t)$, according to its policy $\pi = \{\pi_t\}_{1\le t\le T}$, where $\pi_t : \mathcal{S} \to \Delta(\mathcal{A})$ defines the probability distribution over actions in $\mathcal{A}$ given the observed state $\widetilde{s}_t$. The *action-disruptor* then perturbs this action to $\widetilde{a}_t = D_{\mathsf{a}}(a_t)$, which is then sent to a perturbed environment governed by the *environment-disruptor*, based on the reference — nominal environment (P^0, r^0). The environment then transitions to the next state $s_{t+1} \sim P_t(\cdot \mid s_t, \widetilde{a}_t)$ and provides the reward $r_{t+1}(s_t, \widetilde{a}_t)$, which becomes the input for the observation-disruptor in the next step $t+1$.

Goal. For any Disrupted-MDP, the objective is to learn a policy (action selection rule) $\pi = \{\pi_t\}_{1\le t\le T}$ that maximizes long-term cumulative rewards, represented by the value function $\{V_t^\pi\}_{1\le t\le T} : \mathcal{S} \mapsto \mathbb{R}$:

$$\max_{\pi} V_t^\pi(s) = \mathbb{E}\left[\sum_{k=t}^{T} r_k\left(s_k, \widetilde{a}_k\right) \middle| \pi, (P, r), s_t = s\right]. \tag{1}$$

Here, the expectation is taken over the trajectories generated by executing the policy π under the perturbed transition kernels and reward functions (P, r).

2.2 DISRUPTORS

In Disrupted-MDP, the three types of disruptors represent potential uncertainties or disturbances that impact different stages of the agent-environment interaction process. We introduce each type in detail, along with the available modes and operational frequencies, in the following. We start by introducing the three types of disruptors:

- *Observation-disruptor.* As introduced in Sec. 2.1, an agent's observations may not perfectly reflect the true status of the environment due to factors like sensor noise and time delays. To model this sensing inaccuracy, we introduce an additional module—the observation-disruptor—which determines the agent's observations from the environment: *Agents' observed state $\widetilde{s}_t$:* The observation-disruptor takes the true current state s_t as input and outputs a perturbed state $\widetilde{s}_t = D_{\mathsf{s}}(s_t)$. The agent uses $\widetilde{s}_t$ as input to its policy to select an action; *Agents' observed reward $\widetilde{r}_t$:* The observation-disruptor takes the real immediate reward r_t as input and outputs a perturbed reward $\widetilde{r}_t = D_{\mathsf{r}}(r_t)$. The agent observes $\widetilde{r}_t$ and updates its policy accordingly.
- *Action-disruptor.* The real action a_t chosen by the agent may be altered before or during execution in the environment due to implementation inaccuracies or system malfunctions. The action-disruptor models this perturbation, outputting a perturbed action $\widetilde{a}_t = D_{\mathsf{a}}(a_t)$, which is then executed in the environment for the next step.
- *Environment-disruptor.* Recall that a task environment consists of both the internal dynamic model and the external workspace it interacts with, characterized by its transition dynamics P and reward function r. The environment during training can differ from the real-world environment due to factors such as the sim-to-real gap, human and natural variability, external disturbances, and more. We attribute this potential nonstationarity to an environment-disruptor, which determines the actual environment (P, r) the agent is interacting with at any given moment. These dynamics may differ from the nominal environment (P^0, r^0) that the agent was originally expected to interact with.

In Disrupted-MDP, disruptors affecting various stages of the agent-environment interaction can operate in different modes. We typically consider four common modes found in the robust RL literature, each driven by specific real-world scenarios and robustness requirements. These modes allow the construction of tasks with varying levels of difficulty:

- *Random disturbance: for all disruptors.* Stochastic noise is ubiquitous in sensors, mechanical hardware, and random events, often modeled as random noise added to nominal components in the interaction process (Duan et al., 2016). The noise typically follows a distribution such as Gaussian or uniform. This mode can be applied to all disruptors, affecting the agent's observed state, observed reward, action, and environment.
- *Adversarial disturbance: for all disruptors.* In real-world applications, adversarial disturbances occur when external forces deliberately attempt to degrade the agent's performance. This mode is also relevant when prioritizing safety, ensuring the agent can perform well in worst-case scenarios within certain predefined sets. It can be applied to all three disruptors.
- *Internal dynamic shift: for environment-disruptor.* This mode captures variations in the agent's internal model between training and testing, caused by factors such as the sim-to-real gap, measurement noise, or accidental malfunctions. The environment-disruptor introduces biases to dynamic parameters within a prescribed uncertainty set. For example, the torso length (Fig. 4 (c)) might shift from 0.3 to 0.5.
- *External disturbance: for environment-disruptor.* Nonstationarity in the external workspace can result from variability in the physical world or human behavior, such as changes in wind, friction, or human intervention. The environment-disruptor uses this mode to alter the external conditions of the environment.

In addition to disruption modes, Disrupted-MDP allows disruptors to operate flexibly over time during the interaction process. Disruptors can act at different frequencies, such as step-wise, episode-wise, or at varying intervals.

3 Robust-Gymnasium: A UNIFIED ROBUST RL BENCHMARK

We now introduce our main contribution, a modular benchmark (Robust-Gymnasium) designed for evaluating Robust RL policies in robotics and control tasks. Each task is constructed from three main components: an agent model (the robot object), an environment (the agent's workspace), and a task objective (such as navigation or manipulation). Robust-Gymnasium offers robust RL tasks by integrating various disruptors of different types, modes, and frequencies with these task bases. Not all task bases support every type of disruption. A detailed list of the robust RL tasks implemented in this benchmark is available in Figure 17. In the following sections, we introduce over 60 task bases from eleven sets, outline the design of the disruptors, and describe the construction of a Disrupted-MDP— robust RL tasks.

3.1 TASK AND ENVIRONMENT BASES

Gymnasium-Box2D *(three relative simple control tasks in games).*
These tasks are from Gymnasium (Towers et al., 2024), including three robot models from different games, such as the Bipedal Walker — a 4-joint walking robot designed to move forward and Car Racing — navigating a track by learning from pixel inputs (Parberry, 2017; Brockman et al., 2016).

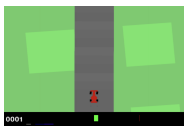

Gymnisium-MuJoCo *(eleven control tasks).*
It includes various robot models, such as bipedal and quadrupedal robots. This benchmark is widely used in various RL problems, including standard online and offline RL, with representative examples like Hopper, Ant, and HalfCheetah (Todorov et al., 2012; Brockman et al., 2016).

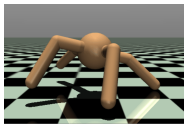

Maze *(two navigation environments).*
Maze comprises environments where an agent must reach a specified goal within a maze (Gupta et al., 2020). Two types of agents are available: a 2-degrees of freedom (DoF) ball (Point-Maze) and a more complex 8-DoF quadruped robot (Ant-Maze) from Gymnasium-MuJoCo. Various goals and maze configurations can be generated to create tasks of varying difficulty.

Fetch *(four tasks for Fetch Mobile Manipulator robot arm).*
Fetch features a 7-degrees of freedom (DoF) Fetch Mobile Manipulator arm with a two-fingered parallel gripper (Plappert et al., 2018). The environment consists of a table with various objectives, resulting in four tasks: Reach, Push, Slide, and PickAndPlace, which involve picking up or moving the objects to specified locations.

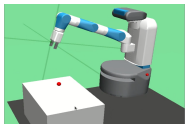

Franka Kitchen *(tasks need long-horizon, multi-task planning for a robot arm).*
This environment is based on a 9-degrees of freedom (DoF) Franka robot situated in a kitchen containing common household items like a microwave and cabinets (Gupta et al., 2020). The task goal is to achieve a specified configuration, which may involve planning and completing multiple sub-tasks. For example, a goal state could have the microwave open, a kettle inside, and the light over the burners turned on.

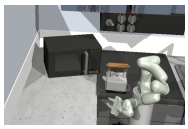

Dexterous Hand *(five dexterous hand manipulation tasks).*
It is based on the Shadow Dexterous Hand — an anthropomorphic 24-DoF robotic hand with 92 touch sensors at palm and phalanges of the fingers (Plappert et al., 2018; Melnik et al., 2021). The tasks involve manipulating various objects, such as a pen, egg, or blocks.

Adroit *(four manipulation tasks for a dexterous hand attached to a free arm).*
This environment features a free arm equipped with a Shadow Dexterous Hand, providing up to 30-DoF (Rajeswaran et al., 2018). The high degree of freedom enables the robot to perform more complex tasks, such as opening a door with a latch (AdroitHandDoor).

HumanoidBench *(four tasks for a high-dimensional humanoid).*
We incorporate four tasks from the recent HumanoidBench (Sferrazza et al., 2024) designed mainly for a Unitree H1 humanoid robot [2], which is equipped with two dexterous Shadow Hands. Specifically, we include two manipulation tasks (push, truck) and two locomotion tasks (reach, slide), all of which require sophisticated coordination among various body parts.

Robosuite *(twelve tasks for various modular robot platforms).*
Robosuite is a popular modular benchmark (Zhu et al., 2020) that supports seven robot arms, eight grippers, and six controller modes. The manipulation tasks are conducted in environments with doors, tables, and multiple robot arms, with goals such as wiping tables or coordinating to transfer a hammer. Additionally, we introduce a new task—MultiRobustDoor—featuring an adversarial arm that impedes another arm's success to test robustness.

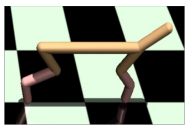

Safety MuJoCo *(nine control tasks with additional safety constraints).*
Built on standard robot models in Gymnasium-MuJoCo, the Safety MuJoCo tasks are designed for scenarios that prioritize both long-term returns and safety. These tasks incorporate safety constraints, such as limiting velocity and preventing robots from falling (Gu et al., 2024).

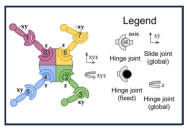

MAMuJoCo *(twelve multi-agent cooperation tasks).*
MAMuJoCo is based on a multi-agent platform from the factorizations of Gymnisium-MuJoCo robot models (Peng et al., 2021). The tasks need to be solved by cooperations of multiple agents. This set of tasks are vulnerable to disturbance like one leg of a quadruped robot is malfunctioning, or all dynamics of legs are contaminated by system noise.

3.2 DISRUPTOR DESIGN: MODES AND FREQUENCIES

Recall that in a Disrupted-MDP, disruptors can operate in various modes and frequencies (timing) and their implementation in Robust-Gymnasium is detailed in this section.

Random disturbance mode. This mode can be applied to all disruptors, enabling the addition of stochastic noise from various distributions to the interaction process. We offer Gaussian distribution $N(\cdot,\cdot)$ and bounded uniform distribution $\mathcal{U}(\cdot,\cdot)$ as default options. For instance, the environment-disruptor can introduce noise to robot dynamics (e.g., mass, torso length) or external factors (e.g., gravity, wind), as shown in Fig. 4. The observation-disruptor can add noise to the observed state and/or reward, namely, $\widetilde{s}_t = s_t + \mathcal{N}(\mu_s, \sigma_s)$ (μ_s and σ_s are the mean and variance) or $\widetilde{s}_t = s_t + \mathcal{U}(a_s, b_s)$ (a_s, b_s are the min and max thresholds). The action-disruptor can also introduce noise to the action sent to the environment.

Adversarial disturbance mode: feature LLM. The disruptor acts as an adversarial agent with restricted power, capable of perturbing variables within an uncertainty set around the nominal values. This mode is applicable to all disruptors; for instance, the observation-disruptor generates a fake state that falls within the prescribed set around the true state, or the environment-disruptor adjusts parameters within a neighborhood of the nominal values. Any algorithm can be applied through this interface to adversarially attack the process.

Notably, in our benchmark, we implement and feature an algorithm leveraging LLM to determine the disturbance. In particular, the LLM is told of the task and uses the current state and reward signal as the input. It directly outputs the disturbed results like a fake state for the agent. See more details in the code 2 in Appendix C.1.

Internal dynamic shift mode of the environment. For tasks in control and robotics, the environment disruptor can alter the robot model, changing the system's internal dynamics. Using Gymnasium-MuJoCo as an example, Fig. 3(b)-(c) depict the consequences of such disruption by altering the Ant robot's head and legs around its original model (Fig. 3(a)).

External disturbance mode of the environment. Additionally, the environment disruptor can modify the task environment by altering properties and configurations within the robot's workspace or

[2] https://www.unitree.com/h1/

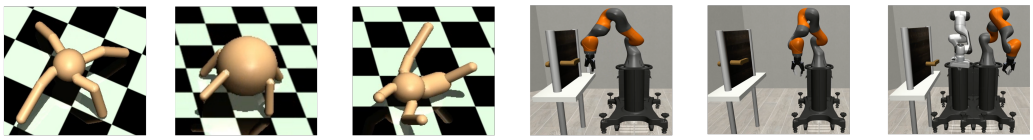

Figure 3: Illustration of two disruption modes of the environment-disruptor: internal dynamic shift and external disturbance.

by introducing abrupt external interventions. For example, in robosuite, Fig. 3(e)-(f) illustrate disrupted tasks compared to the original reference in Fig. 3(d). In these tasks, the environment disruptor changes the distance between the table and the arm, or even introduces an additional arm to actively interfere with the yellow-black robot's ability to accomplish its goal.

Timing of operations for disruptors. We support perturbations occurring at any stage of the process and at different frequencies. Users can choose to apply perturbations at any time step or episode during the training process, or exclusively during testing.

3.3 Constructing robust RL tasks

Robust-Gymnasium is a modular benchmark that offers flexible methods for constructing robust RL tasks through three main steps. First, we select a task base from the eleven options outlined in Sec. 3.1. Second, we choose a disruptor from the observation, action, and environment categories introduced in Sec. 2.2), and specify its operation modes (random disturbance, adversarial disturbance, internal dynamic shift, and external disturbance, as detailed in Sec. 3.2). Finally, we determine the interaction process and frequencies between the disruptor, agent, and environment.

In addition to these basic construction methods, our benchmark supports advanced modes: *A combination of disruptors* allows users to select multiple disruptors, such as an observation-disruptor and an environment-disruptor, to simulate conditions where perception sensors have system noise and external disturbances from human occur; *Varying operation frequencies* enables disruptors to operate intermittently during interactions, either at fixed intervals or in a random pattern to characterize accidental events and uncertainties.

4 Experiments and Analysis

Robust-Gymnasium offers a variety of tasks for comprehensively evaluating the robustness of different RL paradigms. We demonstrate its flexibility by constructing robust RL tasks based on various task bases, incorporating disruptions with different types, modes, and frequencies, and evaluating several SOTA algorithms on these tasks. In addition to benchmarking existing algorithms, we also highlight an adversarial disruption mode that leverages LLMs. Examples of robust RL tasks are shown in Figure 4. More details about the experiments can be found in Appendix E.

Benchmark RL algorithms. Specifically, we benchmark several SOTA algorithms in their corresponding robust RL tasks: **Standard RL:** Proximal Policy Optimization (PPO) (Schulman et al., 2017), Soft Actor-Critic (SAC) (Haarnoja et al., 2018); **Robust RL:** Occupancy-Matching Policy Optimization (OMPO) (Luo et al., 2024), Robust State-Confounded SAC (RSC) (Ding et al., 2024), Alternating Training with Learned Adversaries (ATLA) (Zhang et al., 2021b), and Deep Bisimulation for Control (DBC) (Zhang et al., 2021a); **Safe RL:** Projection Constraint-Rectified Policy Optimization (PCRPO) (Gu et al., 2024), Constraint-Rectified Policy Optimization (CRPO) (Xu et al., 2021); **Multi-Agent RL:** Multi-Agent PPO (MAPPO) (Yu et al., 2022), Independent PPO (IPPO) (De Witt et al., 2020).

Evaluation processes. We mainly focus on two evaluation settings: *In-training*: the disruptor simultaneously affects the agent and environment during both training and testing at each time step. This process is typically used in robotics to address sim-to-real gaps by introducing potential noise during training; 2) *Post-training*: the disruptor only impacts the agent and environment during testing, mimicking scenarios where learning algorithms are unaware of testing variability.

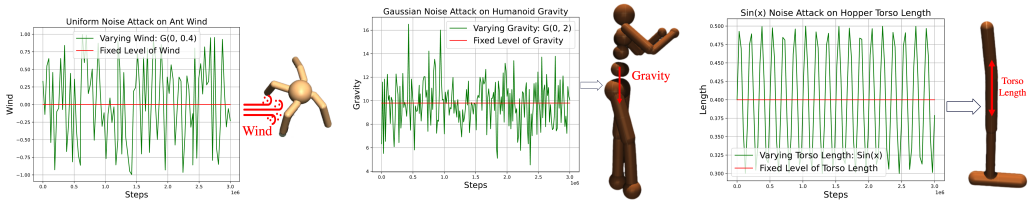

(a) Attack on robot wind (b) Attack on robot gravity (c) Attack on robot torso length

Figure 4: Adversary attack on robot environments, dynamics and shape with different distributions (We can also attack on robot state space, action space and reward signal, etc.).

4.1 Evaluation of standard RL baselines

To begin, we evaluate two types of robust RL tasks: one with an observation disruptor (affecting the agent's observed state) and the other with an action disruptor (affecting the action), both subjected to random disturbances at varying levels. We benchmark the performance of standard RL baselines—PPO (Schulman et al., 2017) and SAC (Haarnoja et al., 2018)—on robust RL tasks based on the representative HalfCheetah-v4 task from Gymnasium-MuJoCo, as partially shown in Figure 5. Here, S=0.1 indicates that the random disturbance over the state follows a Gaussian distribution with a mean of 0 and a standard deviation of 0.1 (resp.0.15). The same applies for A=0.1 or A=0.15. Figures 5 (a)-(b) and Figure 5 (c)-(d) present the results from two different evaluation processes—In-training and Post-training, respectively. The results show that as the disturbance level increases, the performance of the baselines degrades quickly, particularly when the training process is unaware of potential disturbances (as seen in the Post-training results). More experiments, including those using disturbances over reward or the results for SAC, can be found in Appendix B.1.

4.2 Evaluation of robust RL baselines

In this section, we evaluate robust RL tasks using an environment disruptor under two representative modes: internal dynamic shift and external disturbance. The robust RL tasks are based on various task bases, including Ant-v5 and Hopper-v5 from Gymnasium-MuJoCo, as well as DoorCausal-v1 and LiftCausal-v1 from Robosuite, utilizing the In-training evaluation process.

Specifically, Figure 6(a-b) displays the performance of the robust RL baseline OMPO across two tasks with internal dynamic shifts: (a) Ant-v5 with varying gravity and wind strength, and (b) Hopper-v5 with changes to the robot model's shape, including torso and foot length. Experimental settings can be found in (4) and (6) in Appendix C.2. The results indicate that OMPO's performance significantly declines in non-stationary environments compared to stationary conditions without disturbances.

Figures 6(c-d) illustrate the performance of three robust RL baselines (RSC, ATLA, DBC) in two tasks from Robosuite involving disruptions on the environment with external semantic disturbances. In the DoorCausal task, the initial distance of the door from the robot and the height of the door handle are varied in a correlated manner. In the CausalLift task, both the position and color of the object to be lifted are changed together according to specific patterns. RSC demonstrates greater robust-

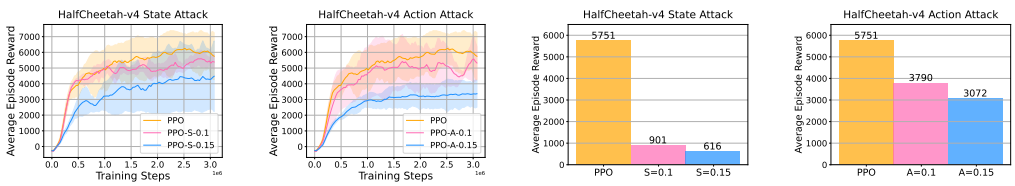

(a) In-training attack (b) In-training attack (c) Post-training attack (d) Post-training attack

Figure 5: Adversary attack on state and action space in robust HalfCheetah-v4 tasks. S denotes attack on state and A denotes attack on action.

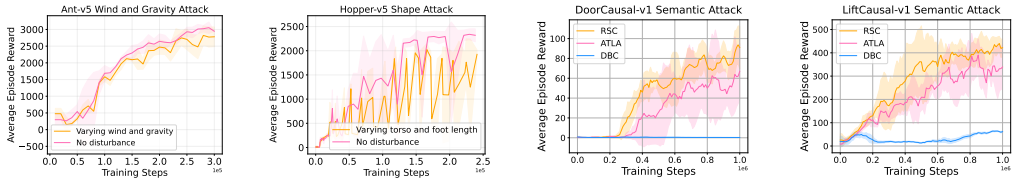

(a) Attack wind & gravity (b) Attack shape (c) Attack position (d) Attack color

Figure 6: (a-b): Internal dynamic shift attacks on Ant-v5 and Hopper-v5 tasks. (c-d): External semantic attacks on Robosuite tasks.

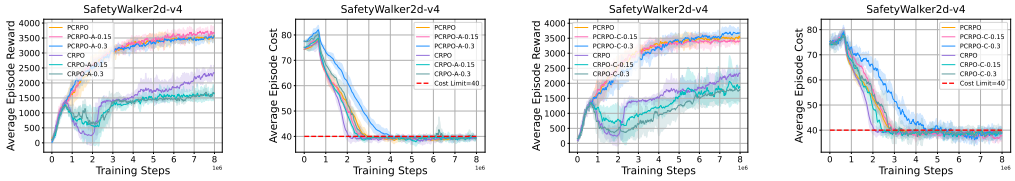

(a) Attack **safe action** (b) Attack **safe action** (c) Attack **cost signal** (d) Attack **cost signal**

Figure 7: Robust safe RL rasks: Random disturbances over either the action or the agent's observed immediate cost feedback.

ness than ATLA and DBC, maintaining stable reward trajectories throughout the training process. However, RSC's training efficiency may need further improvement, as it generates augmentation data during policy learning.

4.3 Evaluation of Safe RL Baselines

Two safe RL baselines, PCRPO (Gu et al., 2024) and CRPO (Xu et al., 2021), are benchmarked on robust safety-critical tasks using the In-training evaluation process. Specifically, we assess two types of robust RL tasks based on Walker2d from Gymnasium-MuJoCo: (a) an action-disruption attacks the agent's action with different levels; (b) the agent's observe immediate safety cost is disturbed in different levels. These attacks follow a Gaussian distribution with a mean of 0 and standard deviations of 0.15 or 0.3 for both the action and the observed cost. The outcomes and safety costs for these tasks are presented in Figures 12(a-b) and Figures 12(c-d), respectively. The performance of CRPO quickly degrades when disruptions occur, while PCRPO demonstrates greater robustness against disturbances in either action or observed cost. Notably, PCRPO's performance under disturbance surpasses its performance without disturbance, suggesting that introducing appropriate disturbances during training may enhance overall performance. Due to space limitations, additional results can be found in Appendix B.2.

4.4 Evaluation of Multi-Agent RL Baselines

We evaluate two MARL baselines: Multi-Agent PPO (MAPPO) (Yu et al., 2022) and Independent PPO (IPPO) (De Witt et al., 2020) on MA-HalfCheetah-v4 from MAMoJoCo under various disruption settings affecting the agents' observed states, actions, and rewards. Using the In-training evaluation process, as shown in Figure 8, we apply disruptions to all agents. The results indicate that the performance of both MAPPO and IPPO degrades accordingly as the disruptions occur. Additionally, we conduct experiments involving **partial disruptions** on a subset of agents within the multi-agent system; further details can be found in Appendix B.3.

4.5 Adversarial Disturbance through LLMs

In addition to benchmarking various existing RL algorithms, this section demonstrates the adversarial disturbance mode by leveraging a featured approach with LLMs. As shown in Figure 9, we evaluate the performance of PPO on Ant-v4 with adversarial disruptions to the agent's observed

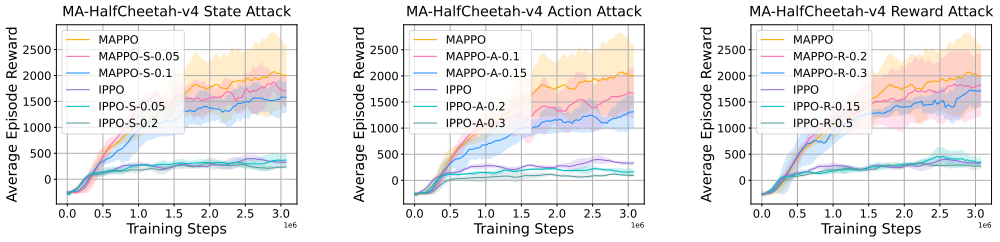

(a) Attack **all agents' state** (b) Attack **all agents' action** (c) Attack **reward signal**

Figure 8: Multi-Agent HalfCheetah-2x3 robustness: training attack on state, action, and reward for all the two agents. S denotes state, A denotes action and R denotes reward.

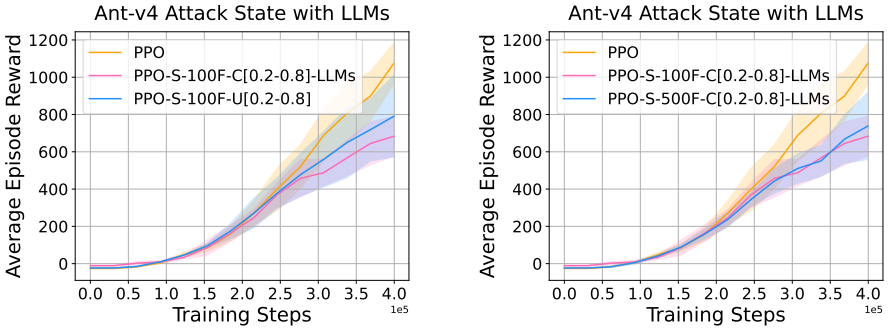

(a) LLMs v.s. uniform (b) Varying frequencies of attacking

Figure 9: LLM-based attacks with different settings.

state. Different attack configurations are employed, including comparisons to uniform noise and testing varying frequencies. Here, "C[0.2–0.8]" indicates that the noise level from the LLM is constrained within the [0.2, 0.8] range; "100F" (resp. "500F") signifies that the agent is attacked every 100 (resp. 500) steps; and "U[0.2–0.8]" represents noise drawn from a uniform distribution $\mathcal{U}(0.2, 0.8)$. The results show that LLM-based attacks lead to a more significant performance drop for PPO compared to that using uniform distribution (Figure 9(a)). Figure (b) examines how varying attack frequencies affect performance, revealing that higher-frequency attacks (PPO-S-100F) result in greater performance degradation. Due to space constraints, additional frequency experiments on other robust tasks based on Gymnasium-MuJoCo using PPO are provided in Appendix B.4.

5 Conclusion

In this work, we introduce Robust-Gymnasium, a unified modular benchmark explicitly designed for robust RL. Unlike existing RL benchmarks, Robust-Gymnasium aims to evaluate the resilience of RL algorithms across a wide range of disruptions. These disruptions include perturbations at every stage of the entire agent-environment interaction process, affecting agent observations, actions, rewards, and environmental dynamics. Robust-Gymnasium provides a comprehensive platform for benchmarking RL algorithms, featuring over 60 diverse task environments across domains such as robotics, multi-agent systems, and safe RL. Additionally, we benchmark various SOTA RL algorithms, including PPO, MAPPO, OMPO, RSC, and IPPO, across a wide array of robust RL tasks in Robust-Gymnasium. The results highlight the deficiencies of current algorithms and motivate the development of new ones. This work represents a significant step forward in standardizing and advancing the field of robust RL, promoting the creation of more reliable, generalizable, and robust learning algorithms.

ACKNOWLEDGMENTS

We extend our sincere appreciation to Weirui Ye, Pieter Abbeel, Banghua Zhu, and Carmelo Sferrazza for their insightful and valuable discussions.

REFERENCES

W Brian Arthur. Designing economic agents that act like human agents: A behavioral approach to bounded rationality. *The American economic review*, 81(2):353–359, 1991.

Kishan Panaganti Badrinath and Dileep Kalathil. Robust reinforcement learning using least squares policy iteration with provable performance guarantees. In *International Conference on Machine Learning*, pp. 511–520. PMLR, 2021.

J Andrew Bagnell, Andrew Y Ng, and Jeff G Schneider. Solving uncertain markov decision processes. 2001.

Dimitris Bertsimas, Melvyn Sim, and Meilin Zhang. Adaptive distributionally robust optimization. *Management Science*, 65(2):604–618, 2019.

Greg Brockman, Vicki Cheung, Ludwig Pettersson, Jonas Schneider, John Schulman, Jie Tang, and Wojciech Zaremba. Openai gym. *arXiv preprint arXiv:1606.01540*, 2016.

Xin Chen, Guannan Qu, Yujie Tang, Steven Low, and Na Li. Reinforcement learning for selective key applications in power systems: Recent advances and future challenges. *IEEE Transactions on Smart Grid*, 13(4):2935–2958, 2022.

Murat Cubuktepe, Nils Jansen, Sebastian Junges, Ahmadreza Marandi, Marnix Suilen, and Ufuk Topcu. Robust finite-state controllers for uncertain pomdps. In *Proceedings of the AAAI Conference on Artificial Intelligence*, volume 35, pp. 11792–11800, 2021.

Mark A Davenport and Justin Romberg. An overview of low-rank matrix recovery from incomplete observations. *IEEE Journal of Selected Topics in Signal Processing*, 10(4):608–622, 2016.

Christian Schroeder De Witt, Tarun Gupta, Denys Makoviichuk, Viktor Makoviychuk, Philip HS Torr, Mingfei Sun, and Shimon Whiteson. Is independent learning all you need in the starcraft multi-agent challenge? *arXiv preprint arXiv:2011.09533*, 2020.

Esther Derman and Shie Mannor. Distributional robustness and regularization in reinforcement learning. *arXiv preprint arXiv:2003.02894*, 2020.

Wenhao Ding, Laixi Shi, Yuejie Chi, and Ding Zhao. Seeing is not believing: Robust reinforcement learning against spurious correlation. In *Thirty-seventh Conference on Neural Information Processing Systems*, 2023a.

Wenhao Ding, Chejian Xu, Mansur Arief, Haohong Lin, Bo Li, and Ding Zhao. A survey on safety-critical driving scenario generation—a methodological perspective. *IEEE Transactions on Intelligent Transportation Systems*, 24(7):6971–6988, 2023b.

Wenhao Ding, Laixi Shi, Yuejie Chi, and Ding Zhao. Seeing is not believing: Robust reinforcement learning against spurious correlation. *Advances in Neural Information Processing Systems*, 36, 2024.

Yan Duan, Xi Chen, Rein Houthooft, John Schulman, and Pieter Abbeel. Benchmarking deep reinforcement learning for continuous control. In *International conference on machine learning*, pp. 1329–1338. PMLR, 2016.

Vineet Goyal and Julien Grand-Clement. Robust markov decision processes: Beyond rectangularity. *Mathematics of Operations Research*, 2022.

Shangding Gu, Bilgehan Sel, Yuhao Ding, Lu Wang, Qingwei Lin, Ming Jin, and Alois Knoll. Balance reward and safety optimization for safe reinforcement learning: A perspective of gradient manipulation. In *Proceedings of the AAAI Conference on Artificial Intelligence*, volume 38, pp. 21099–21106, 2024.

Abhishek Gupta, Vikash Kumar, Corey Lynch, Sergey Levine, and Karol Hausman. Relay policy learning: Solving long-horizon tasks via imitation and reinforcement learning. In *Conference on Robot Learning*, pp. 1025–1037. PMLR, 2020.

Tuomas Haarnoja, Aurick Zhou, Pieter Abbeel, and Sergey Levine. Soft actor-critic: Off-policy maximum entropy deep reinforcement learning with a stochastic actor. In *International conference on machine learning*, pp. 1861–1870. PMLR, 2018.

Songyang Han, Sanbao Su, Sihong He, Shuo Han, Haizhao Yang, and Fei Miao. What is the solution for state adversarial multi-agent reinforcement learning? *arXiv preprint arXiv:2212.02705*, 2022.

Sihong He, Songyang Han, Sanbao Su, Shuo Han, Shaofeng Zou, and Fei Miao. Robust multi-agent reinforcement learning with state uncertainty. *Transactions on Machine Learning Research*, 2023.

Chin Pang Ho, Marek Petrik, and Wolfram Wiesemann. Fast bellman updates for robust MDPs. In *International Conference on Machine Learning*, pp. 1979–1988. PMLR, 2018.

Chin Pang Ho, Marek Petrik, and Wolfram Wiesemann. Partial policy iteration for l1-robust markov decision processes. *Journal of Machine Learning Research*, 22(275):1–46, 2021.

Sandy Huang, Nicolas Papernot, Ian Goodfellow, Yan Duan, and Pieter Abbeel. Adversarial attacks on neural network policies. *arXiv preprint arXiv:1702.02284*, 2017.

Garud N Iyengar. Robust dynamic programming. *Mathematics of Operations Research*, 30(2): 257–280, 2005.

David L Kaufman and Andrew J Schaefer. Robust modified policy iteration. *INFORMS Journal on Computing*, 25(3):396–410, 2013.

Olga Klopp, Karim Lounici, and Alexandre B Tsybakov. Robust matrix completion. *Probability Theory and Related Fields*, 169(1-2):523–564, 2017.

Joseph Peter Kozak, Ruizhe Zhang, Matthew Porter, Qihao Song, Jingcun Liu, Bixuan Wang, Rudy Wang, Wataru Saito, and Yuhao Zhang. Stability, reliability, and robustness of gan power devices: A review. *IEEE Transactions on Power Electronics*, 38(7):8442–8471, 2023.

Zhongyu Li, Xuxin Cheng, Xue Bin Peng, Pieter Abbeel, Sergey Levine, Glen Berseth, and Koushil Sreenath. Reinforcement learning for robust parameterized locomotion control of bipedal robots. In *2021 IEEE International Conference on Robotics and Automation (ICRA)*, pp. 2811–2817. IEEE, 2021.

Qing Liu, Yulan Li, and Katherine Odem-Davis. On robustness of noninferiority clinical trial designs against bias, variability, and nonconstancy. *Journal of biopharmaceutical statistics*, 25(1):206–225, 2015.

Zuxin Liu, Zijian Guo, Zhepeng Cen, Huan Zhang, Jie Tan, Bo Li, and Ding Zhao. On the robustness of safe reinforcement learning under observational perturbations. *arXiv preprint arXiv:2205.14691*, 2022.

Yu Luo, Tianying Ji, Fuchun Sun, Jianwei Zhang, Huazhe Xu, and Xianyuan Zhan. Ompo: A unified framework for rl under policy and dynamics shifts. In *Forty-first International Conference on Machine Learning*, 2024.

A Rupam Mahmood, Dmytro Korenkevych, Gautham Vasan, William Ma, and James Bergstra. Benchmarking reinforcement learning algorithms on real-world robots. In *Conference on robot learning*, pp. 561–591. PMLR, 2018.

Ajay Mandlekar, Yuke Zhu, Animesh Garg, Li Fei-Fei, and Silvio Savarese. Adversarially robust policy learning: Active construction of physically-plausible perturbations. In *2017 IEEE/RSJ International Conference on Intelligent Robots and Systems (IROS)*, pp. 3932–3939. IEEE, 2017.

Shie Mannor, Ofir Mebel, and Huan Xu. Robust mdps with k-rectangular uncertainty. *Mathematics of Operations Research*, 41(4):1484–1509, 2016.

Henrik Marklund, Sang Michael Xie, Marvin Zhang, Akshay Balsubramani, Weihua Hu, Michihiro Yasunaga, Richard Lanas Phillips, Sara Beery, Jure Leskovec, Anshul Kundaje, et al. Wilds: A benchmark of in-the-wild distribution shifts. *arXiv preprint arXiv:2012.07421*, 2020.

Ishita Mediratta, Qingfei You, Minqi Jiang, and Roberta Raileanu. The generalization gap in offline reinforcement learning. *arXiv preprint arXiv:2312.05742*, 2023.

Andrew Melnik, Luca Lach, Matthias Plappert, Timo Korthals, Robert Haschke, and Helge Ritter. Using tactile sensing to improve the sample efficiency and performance of deep deterministic policy gradients for simulated in-hand manipulation tasks. *Frontiers in Robotics and AI*, 8:538773, 2021.

Volodymyr Mnih, Koray Kavukcuoglu, David Silver, Andrei A Rusu, Joel Veness, Marc G Bellemare, Alex Graves, Martin Riedmiller, Andreas K Fidjeland, and Georg Ostrovski. Human-level control through deep reinforcement learning. *Nature*, 518(7540):529–533, 2015.

Janosch Moos, Kay Hansel, Hany Abdulsamad, Svenja Stark, Debora Clever, and Jan Peters. Robust reinforcement learning: A review of foundations and recent advances. *Machine Learning and Knowledge Extraction*, 4(1):276–315, 2022.

OpenAI. Gpt-4 technical report. 2023.

Yuxin Pan, Yize Chen, and Fangzhen Lin. Adjustable robust reinforcement learning for online 3d bin packing. *arXiv preprint arXiv:2310.04323*, 2023.

Ian Parberry. *Introduction to Game Physics with Box2D*. CRC Press, 2017.

Beomsoo Park and Benjamin Van Roy. Adaptive execution: Exploration and learning of price impact. *Operations Research*, 63(5):1058–1076, 2015.

Anay Pattanaik, Zhenyi Tang, Shuijing Liu, Gautham Bommannan, and Girish Chowdhary. Robust deep reinforcement learning with adversarial attacks. *arXiv preprint arXiv:1712.03632*, 2017.

Bei Peng, Tabish Rashid, Christian Schroeder de Witt, Pierre-Alexandre Kamienny, Philip Torr, Wendelin Böhmer, and Shimon Whiteson. Facmac: Factored multi-agent centralised policy gradients. *Advances in Neural Information Processing Systems*, 34:12208–12221, 2021.

Lerrel Pinto, James Davidson, Rahul Sukthankar, and Abhinav Gupta. Robust adversarial reinforcement learning. In *International Conference on Machine Learning*, pp. 2817–2826. PMLR, 2017.

Matthias Plappert, Marcin Andrychowicz, Alex Ray, Bob McGrew, Bowen Baker, Glenn Powell, Jonas Schneider, Josh Tobin, Maciek Chociej, Peter Welinder, et al. Multi-goal reinforcement learning: Challenging robotics environments and request for research. *arXiv preprint arXiv:1802.09464*, 2018.

Wilbert Pumacay, Ishika Singh, Jiafei Duan, Ranjay Krishna, Jesse Thomason, and Dieter Fox. The colosseum: A benchmark for evaluating generalization for robotic manipulation. *arXiv preprint arXiv:2402.08191*, 2024.

You Qiaoben, Xinning Zhou, Chengyang Ying, and Jun Zhu. Strategically-timed state-observation attacks on deep reinforcement learning agents. In *ICML 2021 Workshop on Adversarial Machine Learning*, 2021.

Aravind Rajeswaran, Vikash Kumar, Abhishek Gupta, Giulia Vezzani, John Schulman, Emanuel Todorov, and Sergey Levine. Learning complex dexterous manipulation with deep reinforcement learning and demonstrations. *Robotics: Science and Systems XIV*, 2018.

John Schulman, Filip Wolski, Prafulla Dhariwal, Alec Radford, and Oleg Klimov. Proximal policy optimization algorithms. *arXiv preprint arXiv:1707.06347*, 2017.

Carmelo Sferrazza, Dun-Ming Huang, Xingyu Lin, Youngwoon Lee, and Pieter Abbeel. Humanoidbench: Simulated humanoid benchmark for whole-body locomotion and manipulation. *arXiv preprint arXiv:2403.10506*, 2024.

Elena Smirnova, Elvis Dohmatob, and Jérémie Mary. Distributionally robust reinforcement learning. *arXiv preprint arXiv:1902.08708*, 2019.

Ke Sun, Yi Liu, Yingnan Zhao, Hengshuai Yao, Shangling Jui, and Linglong Kong. Exploring the training robustness of distributional reinforcement learning against noisy state observations. *arXiv preprint arXiv:2109.08776*, 2021.

Zhongchang Sun, Sihong He, Fei Miao, and Shaofeng Zou. Constrained reinforcement learning under model mismatch. *arXiv preprint arXiv:2405.01327*, 2024.

Aviv Tamar, Shie Mannor, and Huan Xu. Scaling up robust MDPs using function approximation. In *International conference on machine learning*, pp. 181–189. PMLR, 2014.

Kai Liang Tan, Yasaman Esfandiari, Xian Yeow Lee, and Soumik Sarkar. Robustifying reinforcement learning agents via action space adversarial training. In *2020 American control conference (ACC)*, pp. 3959–3964. IEEE, 2020.

Chen Tessler, Yonathan Efroni, and Shie Mannor. Action robust reinforcement learning and applications in continuous control. In *International Conference on Machine Learning*, pp. 6215–6224. PMLR, 2019.

Emanuel Todorov, Tom Erez, and Yuval Tassa. Mujoco: A physics engine for model-based control. In *2012 IEEE/RSJ International Conference on Intelligent Robots and Systems*, pp. 5026–5033. IEEE, 2012. doi: 10.1109/IROS.2012.6386109.

Mark Towers, Ariel Kwiatkowski, Jordan Terry, John U Balis, Gianluca De Cola, Tristan Deleu, Manuel Goulão, Andreas Kallinteris, Markus Krimmel, Arjun KG, et al. Gymnasium: A standard interface for reinforcement learning environments. *arXiv preprint arXiv:2407.17032*, 2024.

Amos Tversky and Daniel Kahneman. Judgment under uncertainty: Heuristics and biases: Biases in judgments reveal some heuristics of thinking under uncertainty. *science*, 185(4157):1124–1131, 1974.

Daniel Vial, Sanjay Shakkottai, and R Srikant. Robust multi-agent bandits over undirected graphs. *Proceedings of the ACM on Measurement and Analysis of Computing Systems*, 6(3):1–57, 2022.

Oriol Vinyals, Igor Babuschkin, Wojciech M Czarnecki, Michaël Mathieu, Andrew Dudzik, Junyoung Chung, David H Choi, Richard Powell, Timo Ewalds, Petko Georgiev, et al. Grandmaster level in starcraft ii using multi-agent reinforcement learning. *nature*, 575(7782):350–354, 2019.

Eric M Wolff, Ufuk Topcu, and Richard M Murray. Robust control of uncertain Markov decision processes with temporal logic specifications. In *2012 IEEE 51st IEEE Conference on Decision and Control (CDC)*, pp. 3372–3379. IEEE, 2012.

Bernhard Wymann, Eric Espié, Christophe Guionneau, Christos Dimitrakakis, Rémi Coulom, and Andrew Sumner. Torcs, the open racing car simulator. *Software available at http://torcs. sourceforge. net*, 4(6):2, 2000.

Zikang Xiong, Joe Eappen, He Zhu, and Suresh Jagannathan. Defending observation attacks in deep reinforcement learning via detection and denoising. *arXiv preprint arXiv:2206.07188*, 2022.

Huan Xu and Shie Mannor. The robustness-performance tradeoff in markov decision processes. *Advances in Neural Information Processing Systems*, 19, 2006.

Huan Xu and Shie Mannor. Distributionally robust Markov decision processes. *Mathematics of Operations Research*, 37(2):288–300, 2012.

Tengyu Xu, Yingbin Liang, and Guanghui Lan. Crpo: A new approach for safe reinforcement learning with convergence guarantee. In *International Conference on Machine Learning*, pp. 11480–11491. PMLR, 2021.

Huaxiu Yao, Caroline Choi, Bochuan Cao, Yoonho Lee, Pang Wei W Koh, and Chelsea Finn. Wild-time: A benchmark of in-the-wild distribution shift over time. *Advances in Neural Information Processing Systems*, 35:10309–10324, 2022.

Christopher Yeh, Victor Li, Rajeev Datta, Julio Arroyo, Nicolas Christianson, Chi Zhang, Yize Chen, Mohammad Mehdi Hosseini, Azarang Golmohammadi, Yuanyuan Shi, et al. Sustaingym: Reinforcement learning environments for sustainable energy systems. *Advances in Neural Information Processing Systems*, 36, 2024.

Chao Yu, Akash Velu, Eugene Vinitsky, Jiaxuan Gao, Yu Wang, Alexandre Bayen, and Yi Wu. The surprising effectiveness of ppo in cooperative multi-agent games. *Advances in Neural Information Processing Systems*, 35:24611–24624, 2022.

Tianhe Yu, Deirdre Quillen, Zhanpeng He, Ryan Julian, Karol Hausman, Chelsea Finn, and Sergey Levine. Meta-world: A benchmark and evaluation for multi-task and meta reinforcement learning. In *Conference on robot learning*, pp. 1094–1100. PMLR, 2020.

Amy Zhang, Rowan Thomas McAllister, Roberto Calandra, Yarin Gal, and Sergey Levine. Learning invariant representations for reinforcement learning without reconstruction. In *International Conference on Learning Representations*, 2021a. URL https://openreview.net/forum?id=-2FCwDKRREu.

Huan Zhang, Hongge Chen, Chaowei Xiao, Bo Li, Mingyan Liu, Duane Boning, and Cho-Jui Hsieh. Robust deep reinforcement learning against adversarial perturbations on state observations. *Advances in Neural Information Processing Systems*, 33:21024–21037, 2020.

Huan Zhang, Hongge Chen, Duane S Boning, and Cho-Jui Hsieh. Robust reinforcement learning on state observations with learned optimal adversary. In *International Conference on Learning Representations*, 2021b. URL https://openreview.net/forum?id=sCZbhBvqQaU.

Zhengfei Zhang, Kishan Panaganti, Laixi Shi, Yanan Sui, Adam Wierman, and Yisong Yue. Distributionally robust constrained reinforcement learning under strong duality. *arXiv preprint arXiv:2406.15788*, 2024.

Zhili Zhang, Yanchao Sun, Furong Huang, and Fei Miao. Safe and robust multi-agent reinforcement learning for connected autonomous vehicles under state perturbations. *arXiv preprint arXiv:2309.11057*, 2023.

Ziyuan Zhou and Guanjun Liu. Robustness testing for multi-agent reinforcement learning: State perturbations on critical agents. *arXiv preprint arXiv:2306.06136*, 2023.

Yuke Zhu, Josiah Wong, Ajay Mandlekar, Roberto Martín-Martín, Abhishek Joshi, Soroush Nasiriany, and Yifeng Zhu. robosuite: A modular simulation framework and benchmark for robot learning. *arXiv preprint arXiv:2009.12293*, 2020.

Daniel M Ziegler, Nisan Stiennon, Jeffrey Wu, Tom B Brown, Alec Radford, Dario Amodei, Paul Christiano, and Geoffrey Irving. Fine-tuning language models from human preferences. *arXiv preprint arXiv:1909.08593*, 2019.

Adil Zouitine, David Bertoin, Pierre Clavier, Matthieu Geist, and Emmanuel Rachelson. Rrls: Robust reinforcement learning suite. *arXiv preprint arXiv:2406.08406*, 2024.

A Related Works

Related benchmarks. Despite recent efforts, current robust RL works often evaluate proposed algorithms in overly ideal scenarios, typically involving only one type of disruption at a time. These evaluations are often one-off and limited to a narrow range of tasks in specific domains, such as classical control, robot path planning (Bagnell et al., 2001), autonomous driving (Wymann et al., 2000), investment planning (Mannor et al., 2016), and 3D bin-packing (Pan et al., 2023). A recent robust RL benchmark (Zouitine et al., 2024) introduced six continuous control tasks in Gymnasium-MuJoCo, designed to address environment shifts. However, a clear lack of standardized benchmarks for general robust RL persists, which is essential for the community to evaluate existing efforts and inspire new algorithms. We address this gap by introducing Robust-Gymnasium, a unified modular benchmark that supports over sixty diverse tasks in robotics and control for comprehensive evaluation, and accounting for different types of uncertainty and disruptions across multiple stages of the interaction process.

Moreover, enhancing robustness against environment shifts can be seen as a slight generalization to unseen tasks or environments. A non-exhaustive list of relevant benchmarks includes: a domain generalization benchmark in offline RL (Mediratta et al., 2023), Meta-World for multi-task and meta-RL (Yu et al., 2020), a generalization benchmark for robot manipulation (Pumacay et al., 2024), SustainGym — generalization for sustainable energy systems (Yeh et al., 2024), and others (Marklund et al., 2020; Yao et al., 2022).

Robustness in single-agent RL. Robustness is a key principle in designing RL algorithms, as training processes are often idealized and limited in data and scenarios, while real-world environments are changeable, unpredictable, and highly diverse. An emerging body of work focuses on developing robust RL algorithms that can withstand potential uncertainties, perturbations, and attacks during real-world execution. These efforts can largely be categorized under our unified robust RL framework (Sec. 2), which formulates uncertainty events affecting the agent-environment interaction as behaviors of three types of disruptors. Our proposed Robust-Gymnasium encompasses all types of robust RL tasks within this framework, providing a flexible and comprehensive platform for evaluating and developing robust RL algorithms.

Specifically, prior works typically involve one type of disruptors: Zhang et al. (2020; 2021b); Han et al. (2022); Qiaoben et al. (2021); Sun et al. (2021); Xiong et al. (2022) studied the uncertainty of agent's observed state, controlled by the observation-disruptor who can add restricted noise or perform adversarial attack; Tessler et al. (2019); Tan et al. (2020) considered the robustness w.r.t. the uncertainty of the action, where the action is possibly distorted by the action-disruptor abruptly or smoothly before forwarding to the environment to be executed; A large amount of prior works focus on dealing with the perturbation/shift on the environmental controlled by the environment-disruptor — includes the reward function, the dynamics, or the task itself, ranging from theory (Iyengar, 2005; Xu & Mannor, 2012; Wolff et al., 2012; Kaufman & Schaefer, 2013; Ho et al., 2018; Smirnova et al., 2019; Ho et al., 2021; Goyal & Grand-Clement, 2022; Derman & Mannor, 2020; Tamar et al., 2014; Badrinath & Kalathil, 2021) to applications (Pinto et al., 2017; Pattanaik et al., 2017; Ding et al., 2023a). Besides them, only a few works consider more complex scenarios that more than one disruptors are involved (Mandlekar et al., 2017). See Moos et al. (2022) for a recent review.

Robustness in safe RL and multi-agent RL. Besides the class of standard single-agent RL, robustness in RL algorithms are ubiquitously demanded and has emerges a growing line of works for other RL problems such as partially observable Markov decision processes (POMDPs) (Cubuktepe et al., 2021), safe RL (Liu et al., 2022; Sun et al., 2024; Zhang et al., 2024) and multi-agent RL (Vial et al., 2022; Han et al., 2022; He et al., 2023; Zhou & Liu, 2023; Zhang et al., 2023; 2021b). Additional challenges arise when combining robustness requirements with issues such as safety constraints and strategic interactions, which are often understudied and lack standardized benchmarks for evaluation. Our Robust-Gymnasium not only provides single-agent RL tasks but also encompasses a broader range of RL paradigms, including safe RL and multi-agent RL. This enables a faster and more comprehensive process for designing and evaluating robust RL algorithms across a wider array of RL tasks.

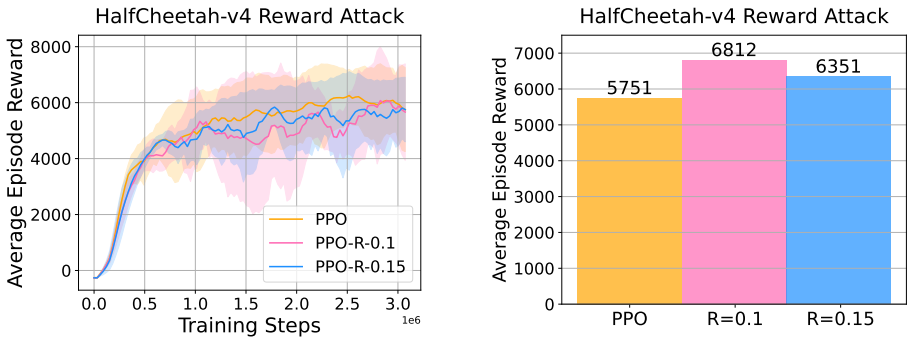

(a) In-Training Attack on Reward

(b) Post-Training Attack on Reward

Figure 10: HalfCheetah-v4 robustness: training attack,reward. Specifically, in experiment (a), we train the PPO algorithm under conditions: without a reward attack, and with a reward attack involving Gaussian noise with standard deviations of 0.1 and 0.5, respectively. In both reward attack scenarios, the noise has a mean of 0, with attack noise standard deviations of 0.1 and 0.15, respectively. In experiment (b), we test the trained PPO models that are attacked during training with reward attacks, using standard deviations of 0.1 and 0.15. After the attack-based training, the models are evaluated in environments without any attacks.

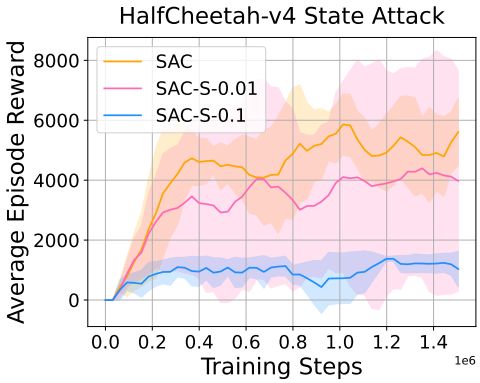

Figure 11: Evaluation SAC robustness on HalfCheetah-v4 tasks.

B Supplementary Experiments and Analysis

B.1 Supplementary for evaluation robustness of standard RL

As shown in Figures 10, they demonstrates the robustness of PPO in the HalfCheetah-v4 environment under various adversarial conditions. Each graph presents the average episode reward across training steps, contrasting the performance of the standard PPO algorithm against its adaptations under diverse adversarial attack parameters. Specifically, the figure for in-Training Attack on Reward (Figure 10 (a)) investigates how modifications to the rewards during training influence the learning performance, employing multiple levels of perturbation. Moreover, the graph for Post-Training Attack on Reward (Figure 10 (b)) assesses how the trained policy withstands alterations to the reward signals post-training. The experimental results suggest that training an RL agent with disturbances and then testing it in ideal environments may lead to improved reward performance in test scenarios. Similarly, we conducted an experiment to evaluate the robustness of another popular RL baseline, SAC. As shown in Figure 11, the performance of SAC degrades under a disturbance attack.

This experiment aids in understanding the stability and robustness of RL policies under adversarial conditions, which is pivotal for deploying these models in real-world scenarios where they may encounter unexpected or adversarial changes in input data.

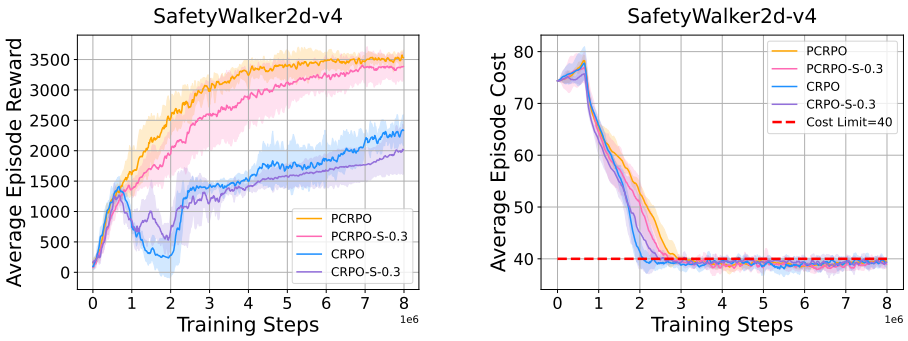

(a) Attack on safe state

(b) Attack on safe state

Figure 12: Robust Safety RL Tasks.

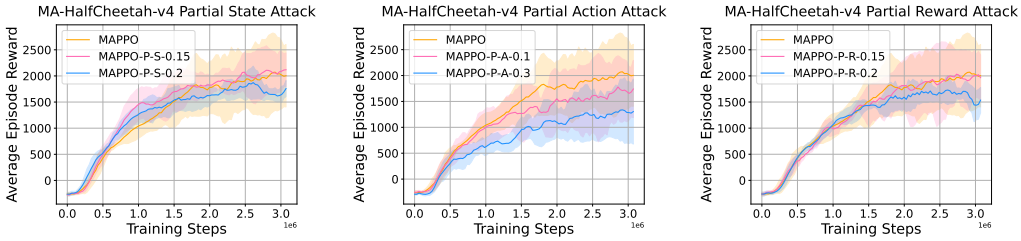

(a) Attack **partial state**

(b) Attack **partial action**

(c) Attack **reward signal**

Figure 13: Multi-Agent HalfCheetah-2x3 robustness: training attack on state, action, and reward for all the two agents. S denotes state, A denotes action and R denotes reward, P denotes partial attacks. Some of agents are attacked with various attack factors.

B.2 Supplementary for evaluation robustness of Safe RL

As depicted in Figures 12(a) and (b), we implement PCRPO (Gu et al., 2024) and CRPO (Xu et al., 2021), SOTA safe RL algorithms, in robust safety-critical tasks. We selected a representative task from robust safe RL to assess the effectiveness of the safe RL algorithm. Specifically, we introduce a disruptor to attack the Walker2d robot's observations during training, as shown in Figures 12(a)-(b). Under these adversarial attacks, the reward performance of both PCRPO and CRPO degrades. The attacks follow a Gaussian distribution with a mean of 0 and standard deviation of 0.3, highlighting the importance of considering disturbance testing before deploying safe RL models in real-world applications.

B.3 Supplementary for evaluation robustness of Multi-Agent RL

As shown in Figures 13 (d), (e), and (f), we investigate partial state, action, and reward attacks on MAPPO, where only a subset of agents or aspects is attacked. These figures show a smaller drop in performance, indicating partial attacks are less harmful compared to full attacks (See Figure 8).

B.4 Frequency Attack

We offer interactive modes that support step-wise, variable interactions between disruptors, agents, and environments, allowing users to apply perturbations at any point in time and in any manner they choose. As shown in Figure 14, the frequency of attacks on tasks is illustrated. Perturbations can occur at various points during the training and testing phases, with different frequencies.

As shown in Figure 15, we provide the results of robustness evaluations on the Ant-v4 task under frequency-based adversarial attacks. The figure consists of two subplots, each examining the performance of PPO-based algorithms under different attack levels and frequencies. In Figure (a),

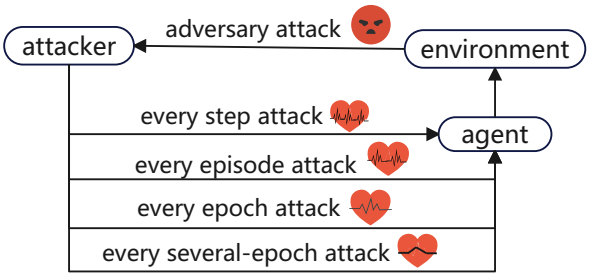

Figure 14: Different levels of robust RL's attack frequency.

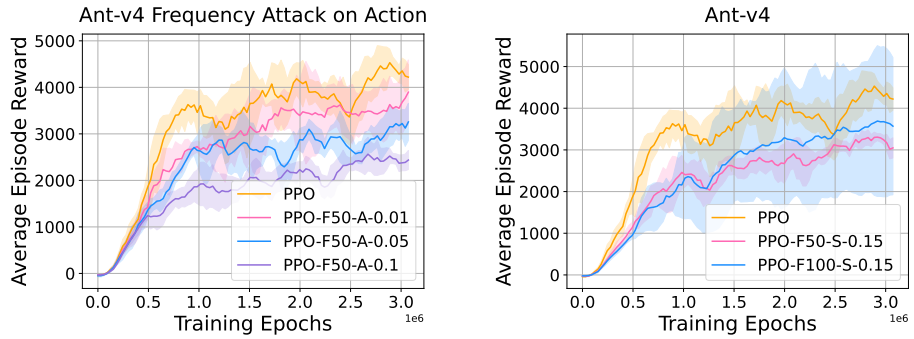

(a) Different level of attacks with same frequency (b) Different level of frequency with same attack

Figure 15: Robust Ant Tasks with Frequency attacks.

we explore the impact of varying attack intensities at a fixed attack frequency (every 50 steps) targeting the agent's actions. As shown, PPO without adversarial intervention achieves the highest episode rewards. However, as the attack intensity increases (PPO-F50-A-0.01, PPO-F50-A-0.05, PPO-F50-A-0.1), the performance declines progressively. The highest intensity attack (PPO-F50-A-0.1) results in the most significant reduction in rewards, indicating a substantial performance drop under stronger attacks. In Figure (b), we examine the effect of varying attack frequencies while keeping the attack intensity constant. Here, PPO-F50-S-0.15 and PPO-F100-S-0.15 represent attacks occurring every 50 and 100 steps, respectively. The results indicate that more frequent attacks (PPO-F50-S-0.15) lead to a larger decline in episode rewards compared to less frequent attacks (PPO-F100-S-0.15). This suggests that attack frequency plays a critical role in determining the robustness of PPO algorithms. Overall, these findings demonstrate that both the intensity and frequency of attacks significantly affect the performance of RL agents, with higher intensities and more frequent attacks causing greater degradation in task performance.

C Other Settings of the Framework

C.1 Benchmark Features

The features of the benchmark are as follows:

High Modularity: It is designed for flexible adaptation to a variety of research needs, featuring high modularity to support a wide range of experiments.

Wide Coverage of : It provides a comprehensive set of tasks to evaluate robustness across different RL scenarios. An overview of the task list is shown in Figure 17.

High Compatibility: It can be seamless and compatible with a wide range of existing environments. An example is shown in Listing 1. Moreover, this benchmark supports vectorized environments, which means it can be useful to enable parallel processing of multiple environments for efficient experimentation.

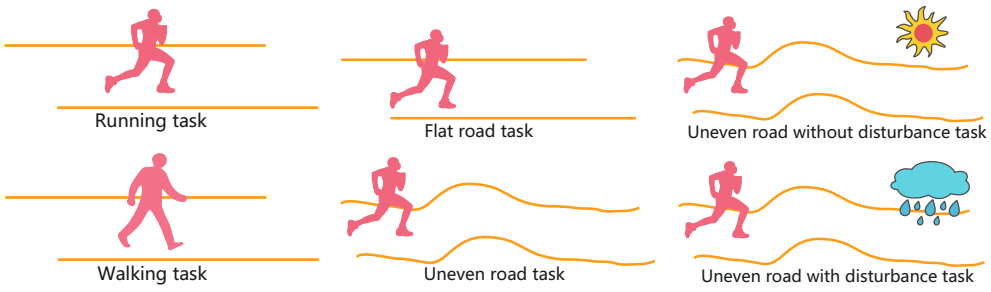

Figure 16: Examples of robust non-stationary tasks (Luo et al., 2024).

```python
from robust_gymnasium.configs.robust_setting import get_config
args = get_config().parse_args()
action = env.action_space.sample()
robust_input = {"action": action, "robust_config": args}
observation, reward, terminated, truncated, info = env.step(robust_input)
```

Listing 1: An example of python interface

Support for New Gym API: It fully supports the latest standards in Gym API, facilitating easy integration and expansion.

Adversarial Attack with LLMs: We feature an approach that leverages LLMs as adversary policies. An example is shown in Listing 2.

```python
prompt = "This is about a robust reinforcement learning setting; we want
    you as an adversary policy. If the current reward exceeds the
    previous reward value, please input some observation noise to disturb
     the environment and improve the learning algorithm's robustness." "
    The noise should be in this area:" +str((args.region_low, args.
    region_high))+ ", the current reward:" + str(reward) + ", the
    previous reward is" + str(self.previous_reward) + "please slightly
    revise the current environment state values:" + str(observation) + ",
     just output the revised state with its original format" "do not
    output any other things."
prompt_state = gpt_call(prompt)
observation = prompt_state
```

Listing 2: An example of LLMs for robust learning

C.2 Robust Non-Stationary Tasks:

Inspired by OMPO (Luo et al., 2024), we provide various task settings to evaluate policy robustness, as illustrated in Figure 16. During policy learning, we introduce adversarial attacks during walking or running tasks by altering robot dynamics and environmental conditions. For instance, we stochastically adjust the robot's gravity and the environment's wind speed, introducing uncertain disturbances during policy learning. Additionally, we stochastically modify the robot's physical shape throughout the learning process to test and enhance policy robustness.

Specifically, in non-stationary Ant-v5 Tasks, during each step, we introduce noise into the agent's dynamics by attacking factors like the Ant robot's gravity and the wind speed in the robot's environment. As demonstrated in Equation (2) for attacks at initial and training steps, we introduce deterministic perturbations to the Ant robot, such as variations in gravity and environmental wind speed, the pseudo code is shown in Listing 3. Furthermore, Equation (3) is for initial noise, and Equation (4) is for noise during training we use these Equarions to consider the incorporation of stochastic disturbances into the Ant robot model, again including factors like gravity fluctuations and wind speed variations, the pseudo code is shown in Listing 4. Apart from wind and gravity disturbances, we also investigate the robot shape disturbances during policy learning, as shown in Equations (5)-(8), and an example of pseudo code is shown in Listing 5.

At the initial and training steps, if we choose non-stationary attack as deterministic noise,

$$\text{Ant deterministic noise} = \begin{cases} \text{Gravity} = 14.715, \\ \text{Wind} = 1.0. \end{cases} \tag{2}$$

if we choose non-stationary attack as stochastic noise,

$$\text{Ant and Humanoid stochastic noise at initial steps} = \begin{cases} \text{Gravity} \sim \text{Uniform}(9.81, 19.82), \\ \text{Wind} \sim \text{Uniform}(0.8, 1.2). \end{cases} \tag{3}$$

During training steps, if we choose non-stationary attack as stochastic noise, where i_{episode} denotes the training step number,

$$\text{Ant and Humanoid noise during training} = \begin{cases} \text{Gravity} = 14.715 + 4.905 \cdot \sin\left(0.5 \cdot i_{\text{episode}}\right), \\ \text{Wind} = 1.0 + 0.2 \cdot \sin\left(0.5 \cdot i_{\text{episode}}\right). \end{cases} \tag{4}$$

$$\text{Walker stochastic noise at initial steps} = \begin{cases} \text{Torso Length} \sim \text{Uniform}(0.1, 0.3), \\ \text{Foot Length} \sim \text{Uniform}(0.05, 0.15). \end{cases} \tag{5}$$

$$\text{Walker Stochastic noise} = \begin{cases} \text{Torso Length} = 0.2 + 0.1 \sin(0.3 \cdot i_{\text{episode}}) \\ \text{Foot Length} = 0.1 + 0.05 \sin(0.3 \cdot i_{\text{episode}}) \end{cases} \tag{6}$$

$$\text{Hopper stochastic noise at initial steps} = \begin{cases} \text{Torso Length} \sim \text{Uniform}(0.3, 0.5), \\ \text{Foot Length} \sim \text{Uniform}(0.29, 0.49). \end{cases} \tag{7}$$

$$\text{Walker Stochastic noise} = \begin{cases} \text{Torso Length} = 0.4 + 0.1 \cdot \sin(0.2 \cdot i_{\text{episode}}), \\ \text{Foot Length} = 0.39 + 0.1 \cdot \sin(0.2 \cdot i_{\text{episode}}). \end{cases} \tag{8}$$

```python
if config.deter_noise:
    gravity = 14.715
    wind = 1.
else:
    gravity = np.random.uniform(9.81, 19.82)
    wind = np.random.uniform(0.8, 1.2)
```

Listing 3: An example of Non-stationary Ant python code for initial steps.

```python
if config.deter_noise:
    gravity = 14.715
    wind = 1.
else:
    gravity = 14.715 + 4.905 * np.sin(0.5 * i_episode)
    wind = 1. + 0.2 * np.sin(0.5 * i_episode)
```

Listing 4: An example of Non-stationary Ant python code for training steps.

```python
if config.deter_noise:
    torso_len = 0.2
    foot_len = 0.1
else:
    torso_len = 0.2 + 0.1 * np.sin(0.3 * i_episode)
    foot_len = 0.1 + 0.05 * np.sin(0.3 * i_episode)
```

Listing 5: An example of Non-stationary Walker python code for training steps.

D REPRESENTATIVE EXAMPLES OF USING Robust-Gymnasium

In this section, we present an overview of the task environments, as illustrated in Figure 17. Additionally, we show some robustness-focused tasks, detailed in Tables 1-8.

Class of Tasks \ disturbance types			Observed state/ Observed reward/ Action		Environment
			random	Adversarial (LLM)	Dynamics or disturbance
Single-agent	Control	Box2D			
		Gymnasium-MuJoCo			☑
	Robot Navigation	Maze			
	Robot Manipulation (diverse robots and tasks)	Dexterous Hand			
		Adroit Hand			
		Fetch Manipulation			
		Franka Kitchen			
		robosuite			☑
		Humanoid			
Safety	Safety MuJoCo				
Multi-agent	MAMuJoCo				

Figure 17: An overview of task environments and supported disruptions in Robust-Gymnasium.

Table 1: A List of Examples for Robustness in MuJoCo Tasks

Tasks\Robust type	Robust State	Robust Action	Robust Reward	Robust Dynamics
Ant-v2-v3-v4-v5	✓	✓	✓	✓
HalfCheetah-v2-v3-v4-v5	✓	✓	✓	✓
Hopper-v2-v3-v4-v5	✓	✓	✓	✓
Walker2d-v2-v3-v4-v5	✓	✓	✓	✓
Swimmer-v2-v3-v4-v5	✓	✓	✓	✓
Humanoid-v2-v3-v4-v5	✓	✓	✓	✓
HumanoidStandup-v2-v3-v4-v5	✓	✓	✓	✓
Pusher-v2-v3-v4-v5	✓	✓	✓	✓
Reacher-v2-v3-v4-v5	✓	✓	✓	✓
InvertedPendulum-v2-v3-v4-v5	✓	✓	✓	✓

Table 2: A List of Examples for Robustness in Box2d Tasks

Tasks \Robust Type	Robust State	Robust Action	Robust Reward
CarRacing-v2	✓	✓	✓
LunarLanderContinuous-v3	✓	✓	✓
BipedalWalker-v3	✓	✓	✓
LunarLander-v3 (Discrete Task)	✓	✓	✓

E EXPERIMENT SETTINGS

We deploy several SOTA baselines in our benchmark to evaluate their robustness across various challenging scenarios. The implementation parameters associated with these methods are provided in Tables 9-13.

Table 3: A List of Examples for Robustness in Robosuite Tasks

Tasks \Robust Type	Robust State	Robust Action	Robust Reward
Lift	✓	✓	✓
Door	✓	✓	✓
NutAssembly	✓	✓	✓
PickPlace	✓	✓	✓
Stack	✓	✓	✓
Wipe	✓	✓	✓
ToolHang	✓	✓	✓
TwoArmLift	✓	✓	✓
TwoArmPegInHole	✓	✓	✓
TwoArmHandover	✓	✓	✓
TwoArmTransport	✓	✓	✓
MultiDoor	✓	✓	✓

Table 4: A List of Examples for Robustness in Safety Tasks

Tasks \Robust Type	Robust State	Robust Action	Robust Reward
SafetyAnt-v4	✓	✓	✓
SafetyHalfCheetah-v4	✓	✓	✓
SafetyHopper-v4	✓	✓	✓
SafetyWalker2d-v4	✓	✓	✓
SafetySwimmer-v4	✓	✓	✓
SafetyHumanoid-v4	✓	✓	✓
SafetyHumanoidStandup-v4	✓	✓	✓
SafetyPusher-v4	✓	✓	✓
SafetyReacher-v4	✓	✓	✓

Table 5: A List of Examples for Robustness in Adroit Hand Tasks

Tasks \Robust Type	Robust State	Robust Action	Robust Reward
AdroitHandDoor-v1	✓	✓	✓
AdroitHandHammer-v1	✓	✓	✓
AdroitHandPen-v1	✓	✓	✓
AdroitHandRelocate-v1	✓	✓	✓

Table 6: A List of Examples for Robustness in Hand Manipulation Tasks

Tasks \Robust Type	Robust State	Robust Action	Robust Reward
HandManipulateEgg_BooleanTouchSensors-v1	✓	✓	✓
HandReach-v2	✓	✓	✓
HandManipulateBlock-v1	✓	✓	✓
HandManipulateEgg-v1	✓	✓	✓
HandManipulatePen-v1	✓	✓	✓

Table 7: A List of Examples for Robustness in Fetch Manipulation Tasks

Tasks \Robust Type	Robust State	Robust Action	Robust Reward
FetchPush-v3	✓	✓	✓
FetchReach-v3	✓	✓	✓
FetchSlide-v3	✓	✓	✓
FetchPickAndPlace-v3	✓	✓	✓

Table 8: A List of Examples for Robustness in Multi-Agent Tasks

Tasks \Robust Type	Robust State	Robust Action	Robust Reward
MA-Ant-2x4, 2x4d, 4x2, 4x1	✓	✓	✓
MA-HalfCheetah-2x3, 6x1	✓	✓	✓
MA-Hopper-3x1	✓	✓	✓
MA-Walker2d-2x3	✓	✓	✓
MA-Swimmer-2x1	✓	✓	✓
MA-Humanoid-9—8	✓	✓	✓
MA-HumanoidStandup-v4	✓	✓	✓
MA-Pusher-3p	✓	✓	✓
MA-Reacher-2x1	✓	✓	✓
Many-MA-Swimmer-10x2, 5x4, 6x1, 1x2	✓	✓	✓
Many-MA-Ant-2x3, 3x1	✓	✓	✓
CoupledHalfCheetah-p1p	✓	✓	✓

Parameters	Value	Parameters	Value
buffer size	4096	hidden size	[64, 64]
lr	3e-4	gamma	0.99
epoch	100	steps per epoch	30000
steps per collect	2048	repeat per collect	10
batch size	64	training num	8
testing num	10	rew norm	True
vf coef	0.25	ent coef	0.0
gae lambda	0.95	bound action clip	clip
lr decay	True	max grad norm	0.5
eps clip	0.2	dual clip	None
value clip	0	norm adv	0
recompute adv	0		

Table 9: Parameter values used for PPO (Schulman et al., 2017), MAPPO (Yu et al., 2022) and IPPO (De Witt et al., 2020) in experiments.

Parameters	Value	Parameters	Value
buffer size	4096	hidden size	[64, 64]
actor lr	1e-3	critic lr	1e-3
gamma	0.99	tau	0.005
alpha	0.0.2	auto alpha	False
epoch	100	steps per epoch	30000
steps per collect	2048	update per step	1
start time step	10000	n step	1
batch size	64	training num	8
testing num	10		

Table 10: Parameter values used for SAC (Haarnoja et al., 2018) in the experiment.

Parameters	Value	Parameters	Value
start steps	5000	num steps	300000
eval	True	eval episode	10
eval times	10	local reply size	1000
gamma	0.99	tau	0.005
lr	3e-4	alpha	0.2
batch size	256	update per step	3
target update interval	2	hidden size	256
gail batch	256	exponent	1.5
tomac alpha	1e-3	reward max	1

Table 11: Parameter values used for OMPO (Luo et al., 2024) in non-stationary MuJoCo experiments.

Parameters	Value	Parameters	Value
image obs	False	actor lr	3e-4
critic lr	1e-3	gamma	0.99
tau	5e-3	alpha	0.1
auto alpha	True	alpha lr	3e-4
hidden size	[256, 256, 256]	n steps	4
buffer size	1e6	step per epoch	1e4
step per collect	20	batch size	128
start time step	0	exploration noise	0
horizon	300	camera	agentview
height	128	width	128
encoder type	mlp	training num	10
test num	10	sigma	0.01
bound	0.01	augmented ratio	0.5
vae sigma	1.0	control frequency	20

Table 12: Parameter values used for RSC (Ding et al., 2024) in the causaldoor/causallift experiments; for DBC (Zhang et al., 2021a), based on above parameters, transition model type is probabilistic, encoder feature dim is 256, encoder lr is 1e-4, decoder lr is 1e-4, bisim coef is 0.5, log std min is -10, log std max is 2; for ATLA (Zhang et al., 2021b), policy update max is 100, adv update max is 100, and adv eps is 0.01.

Parameters	Value	Parameters	Value
gamma	0.995	hidden layer dim	64
cost limit	0.04	slack bound	5e-3
exploration iteration	40	epoch	500
tau	0.97	l2 reg	1e-3
max kl	1e-2	damping	1e-1
batch size	150000	gradient wr	0.4
gradient wc	0.6		

Table 13: Parameter values used for PCRPO (Gu et al., 2024) and CRPO (Xu et al., 2021) in the safety experiments.